IEEE Access
Multidisciplinary | Rapid Review | Open Access Journal

Received July 5, 2017, accepted July 30, 2017, date of publication August 8, 2017, date of current version October 12, 2017.

Digital Object Identifier 10.1109/ACCESS.2017.2737547

General Energy Filters for Power Smoothing, Tracking and Processing Using Energy Storage

ZUANHONG YAN AND XIAO-PING ZHANG, (Senior Member, IEEE)
Department of Electronic, Electrical and System Engineering, University of Birmingham, Birmingham B15 2TT, U.K.
Corresponding author: Xiao-Ping Zhang (x.p.zhang@bham.ac.uk)

This work was supported by EPSRC under Grant EP/L017725/1 and Grant EP/N032888/1

ABSTRACT In the signal processing, active signal filters are commonly used to filter out the zero-average high-frequency components of a signal. In the power system, the power filters are used to filter and control the harmonics in voltages and current waveforms in the concept of power quality. In this paper, we introduce energy filters to filter and control the undesirable frequency components of power flow waveforms in the concept of energy quality. In contrast to the power filters, a family of general energy filters (GEFs) using energy storage is proposed, which virtually work as low-pass filters of power flow and can smooth, track, and process the power flow, as the power filters do with the current and voltage waveforms. In order to illustrate the GEF, the mainstream electrical energy storage (EES) systems are briefly reviewed and classified, and a general model of the EES is developed accordingly. Then, the series, parallel, and series–parallel GEF in the first and second order are proposed, and the focuses are laid on their topologies and controls. Time-domain demonstrations of the GEF based on different implementations are presented on RTDS. Bode plots of the proposed GEF are also obtained through simulations. Finally, key factors in designing GEF for practical applications are briefly discussed.

INDEX TERMS Energy filter, energy quality, electrical energy storage, power smoothing, power filter, power quality.

NOMENCLATURE

u_C	Capacitor voltage
i_C	Capacitor current
C	Capacitance
i_L	Inductor current
u_L	Inductor voltage
L	Inductance
ω	Rotor speed
T	Torque
J	Flywheel inertia
p_C	Compressed air pressure
V_φ	Volume flow
N_A	Avogadro constant
V_0	Container volume
R	Gas constant
ρ_A	Gas density
T_A	Environmental temperature
h	Water height
G_φ	Gravity flow
ρ_w	Water density
g	Gravitational acceleration
S	Cross-sectional area

I. INTRODUCTION

The balance of the power generation and consumption is a key problem of the power system operation and control. With the increasing penetration of intermittent renewable power sources, to achieve this balance is becoming more challenging. This paper proposes a solution to this problem called the general energy filter (GEF).

A. BACKGROUND AND MOTIVATIONS

Unlike conventional power stations, for most of the renewable power sources, the prime mover power is fluctuating and uncontrollable since the maximum power take-off control is applied in most cases. This power fluctuation comes in two time scales: the long-term (hours to days) and the short-term (seconds). The long-term power fluctuation is the change of the average level of power from hours to a day, which is handled by the secondary frequency regulation of the system and the optimized operations of long-term electrical energy storage (EES) as those proposed in previous papers [1]–[3]. The short-term power fluctuation, on the other hand, is the change of real-time power in the time scale of seconds. For example, wave power fluctuates heavily during every wave period (5 $\sim$ 12s), through its

long-term power level is very steady compared with wind and solar [4]. This fluctuation causes frequency change, voltage flicker, thermal excursions, and undermines the transient stability of the system such as the PV [5] and wave power [6] generation. Thus, it must be treated carefully at the common coupling point (PCC). Despite of the power sources, real-time power fluctuations also occur at the consumer side with pulsating loads. An example is the electrical power system on warships, where the power sources are stable and fully controllable but the loads including the weapon systems and the electromagnetic catapult are sharply pulsating [7], [14]. Operation of Microgrids involving pulsating loads and PV sources was studied in [8]. In order to achieve a stable and reliable operation of these systems, smoothing the consumer-side power fluctuation is desirable especially when the local grid is not so strong.

To address the challenges of power source/load fluctuations, EES control systems are considered to be promising solutions. The topic of EES control has been studied in previous papers. With a given power reference, different methods for reference tracking were discussed and compared in [9]. More importantly, another branch of the problem is how to determine the power reference itself, which was not covered in the literature, i.e. [9] on the reference tracking. For long-term applications, the power reference determination was usually studied as a multi-objective optimization problem. Optimized energy storage operation using a mixed-integer-linear program on an hour-to-hour basis was presented in [1]. Similar approaches were used in [2] to improve the performances and minimize the electricity cost in microgrids. Reference [3] proposed a semi-Markov model to predict the variation of PV power for the energy storage control through a day. However, these long-term problem studies have not considered the real-time control of EES for power smoothing or frequency/voltage support.

On the other hand, the reference determination of short-term EES has been widely studied based on different applications and different control and power estimation methods. Output power smoothing of wind farm was studied in [10] using adaptive controlled superconducting magnetic energy storage (SMES) system, in [11] using a fuzzy neural network control of battery energy storage (BESS), and in [12] using the self-inertia of turbine and the DC-link capacitor of the DFIG itself. This problem was studied together with the fault ride-through (FRT) of wind farms using superconducting fault current limiter (SFCL) and SMES in [13]. Reference [14] proposed a model predictive control of BESS to smooth the power fluctuation in a weak ship grid. Reference [15] studied the power smoothing of marine current generation by controlling supercapacitors. The applications of power smoothing control using the electric vehicle charging stations was reported in [16]. However, none of the above studies has established a clear transfer function between the input and output power.

B. CONTRIBUTIONS AND PAPER ARRANGEMENTS

Mathematically, real-time power smoothing control can be analogous to signal filtering using active filters, which are common tools used in signal processing when the high-frequency components need to be removed from the signals. This is similar with the process of power smoothing of fluctuating sources and pulsating loads, in which the high-frequency fluctuating components are to be removed from the power flow, while the low-frequency components would be left with the same long-term average value. On the other hand, using passive filters, or known as the power filters, to remove voltage or current harmonics in the power system is a well-known practice, but these "power filters" do not filter power fluctuations carried in the fundamentals. Despite of the mature applications of active signal filters in the signal processing and passive power filters in the voltage/current waveform improvements, the concept of filters has never been adopted to power smoothing control.

In this paper, a family of controlled EES systems is proposed which virtually work as low-pass filters of the power flow carried on the fundamental frequency. We propose the name of general energy filter (GEF) for power flows in order to avoid the confusion with the conventional power filters (for currents and voltages waveforms). The proposed control methods are independent from the selection EES hardware, and the whole system can be implemented based on most of the mainstream storage devices including batteries, supercapacitors, flywheels, superconducting magnetic energy storage (SMES), etc. Like an active signal filter, the energy filters have their transfer functions, Bode plots, and cut-off frequencies. It's particularly useful to smooth short-term power fluctuations or to track an unknown input power without measuring it. Like using the conventional active filters to process signals or power filters to improve power quality of voltage and current waveforms, the proposed GEF are able to process the power flow waveforms and improve the Energy Quality of power flow waveforms.

The rest of this paper is arranged as follows. Section II presents a brief review on the mainstream EES solutions and develops a general model to describe them. Section III proposes the family of GEF in terms of their different topologies and order. In section IV, applications of GEF based on different EES are demonstrated using time-domain simulations on the RTDS platform. In section V, the Bode plots of both 1st and 2nd order GEF are drawn based on simulated data and compared with the theoretical results. Section VI briefly discusses the design process of GEF. Finally, section VII concludes the study.

II. CLASSIFICATION AND GENERAL MODEL OF ENERGY STORAGE

Unlike signals which can be created or eliminated from nowhere, energy obey the law of conservation, thus, EES is a necessary physical part of an energy filter to allow the high-frequency power flow exchanges with the input power. This

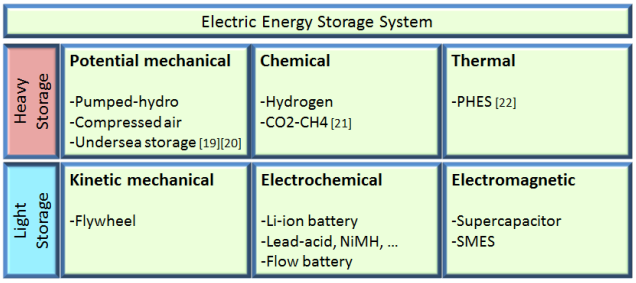

FIGURE 1. Electric energy storage classification.

section firstly reviews and classifies different EES in terms of their energy forms and characteristics. Secondly, a general model is developed based on their similarities to prepare for the energy filter development.

A. CLASSIFICATION OF ELECTRIC ENERGY STORAGE SYSTEMS

In this paper, the current EES solutions are classified into six groups: potential mechanical, kinetic mechanical, electromagnetic, electrochemical (battery), chemical, and thermal energy storage. They are further classified into heavy and light storage systems according to their different characteristics and compatibility with GEF.

Comprehensive reviews and comparative studies of EES are presented in [17] and [18]. For mechanical potential storage, despite of the pumped-hydro storage (PHS) and the compressed air storage (CAES), the undersea storage is an emerging EES whose details are discussed in [19] and [20] with an expected cycle efficiency close to PHS. For chemical storage, its latest progress of creating CH4 from CO2 using electric power is reported in [21]. Thermal energy storage (TES) for large-scale electric applications is studied in [22] with an efficiency approaches 67%.

For the development of GEF, there are 3 coefficients of EES we are particularly interested: cycle efficiency of energy conversion, response time, and rated capacity. For the heavy storage, PHS is of the highest cycle efficiency up to 85%, while the typical number is about 30% $\sim$ 70% for others. It takes minutes for the heavy storage to respond. By comparison, the cycle efficiency of light storage is easily over 90% and up to 95% $\sim$ 97%. The response time is milliseconds to one second. The rated capacity is about 10MWh $\sim$ 3GWh for the heavy storage, while this is about 0.1kWh $\sim$ 8MWh for the light storage [17].

The differences between the heavy and light storage can be summarized as follows. Heavy storage is usually with larger rated capacity, slower response time, and lower cycle efficiency of energy conversion. Particularly, it is inconvenient for chemical storage to achieve a bi-directional power flow with the electrical system. Comparatively, light storage is small-scaled, faster, with higher cycle efficiency, and more friendly to the bi-directional power flow operations with the electrical system. Due to these characteristics, these two kinds are suitable for different applications. Heavy storage is suitable for large-scale and long-term energy storage to achieve secondary frequency regulation, peak load leveling, and economic operations of the grid. Light storage is suitable for short-term energy storage to improve the power quality on the PCC, synthesize virtual inertia, and suppress the power oscillations. In these applications, due to the rapid change of the power flow directions and special demands of control characteristics, high efficiency and fast response of the EES are particularly required. As presented later in this paper, though PHS and CAES are also included in the general model, GEF is especially compatible with the light storage.

B. GENERAL MODEL OF ENERGY STORAGE

Based on the energy storage classification presented above, this subsection proposes a general model covering pumped-hydro, compressed air, and the light storage.

Generally, the energy storage process could be described using 3 variables: potential variable σ, flow variable φ, and the inertia of potential K_σ. The actual physical variables in each EES play these 3 roles are listed in Table I. The storage level α is defined as the ratio of the real-time energy stored in EES over the rated stored energy E_0. For all except the battery, we have

$$\varphi = K_\sigma \frac{d\sigma}{dt} \tag{1}$$

$$P_S = \sigma \cdot \varphi \tag{2}$$

where P_S is the power converted from the electrical system and injected to the energy storage.

For the light storage (flywheel, supercapacitor and SMES), the relationship described by eq. (1) is straightforward.

For the compressed air storage, despite of the container volume V_0, the inertia K_σ is also a function of the gas density ρ_A and the environmental temperature T_A, which may change marginally on an hour-to-hour basis. The inertia of the pumped-hydro storage is proportional to the cross-sectional area of the reservoir on the current water level, which is not necessarily a constant when the water level changes. These factors bring non-linearity and parameter uncertainty into the model of heavy storage that requires special considerations.

For the batteries, there is no clear physics which plays as the inertia. Its rated stored energy, known as the storage capacity, is provided by the manufacture. Its storage level is a function of the state of charge (SoC) as shown in eq. (3), where a_1 and a_0 are two constants determined by open-circuit experiments [23]. Usually, we have $a_1 \ll a_0$, so in this case the storage level of a battery is approximately equal to SoC, especially when it is not too low.

$$\alpha_{Battery} = f_\alpha(SoC) = \frac{a_1 SoC^2 + 2a_0 SoC}{a_1 + 2a_0} \approx SoC \tag{3}$$

The power flow of any energy storage system (EES) listed in Table I could be described by Fig. 2, where η is the energy conversion efficiency and P_δ is the storage loss. Accordingly,

TABLE 1. General variables in each kind of EES.

Energy storage Type	Potential σ	Flow φ	Inertia of potential K_σ	Rated stored energy E_0	Storage level α
Supercapacitor	u_C	i_C	C	$\frac{1}{2}K_\sigma\sigma_0^2$	$\frac{\sigma^2}{\sigma_0^2}$
SMES	i_L	u_L	L		
Flywheel	ω	T	J		
Compressed air	p_C	V_φ	$(N_A V_0)/(R\rho_A T_A)$		
Pumped-hydro	h	G_φ	$\rho_w g S$		
Battery	electrochemical potential	electron/ion flow rate		E_0	$f_\alpha(SoC) \approx SoC$

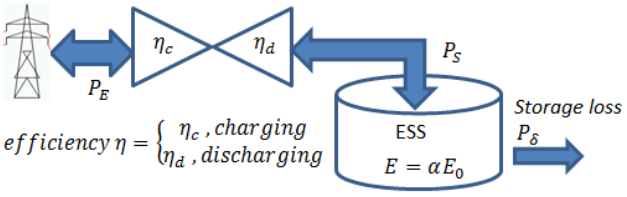

FIGURE 2. Power flow of an EES considered in this study.

we have

$$\frac{dE}{dt} = E_0\frac{d\alpha}{dt} = P_S - P_\delta \tag{4}$$

$$P_S = \begin{cases} \eta_c \cdot P_E & charging \\ \frac{1}{\eta_d} \cdot P_E & discharging \end{cases} \tag{5}$$

Practically, P_δ is small enough that could be reasonably ignored. When it is ignored, by applying eq. (1)(2) into (4), we have

$$E = \int \sigma \cdot K_\sigma \frac{d\sigma}{dt}dt = \frac{1}{2}K_\sigma\sigma^2 \tag{6}$$

Thus, for all EES listed in table I except the battery, the storage level α is proportional to σ^2 when the inertia K_σ is treated as a constant.

Eq. (4)(5) and the storage level α expressed in table I combined build the general model of an energy storage system, based on which the general energy filters (GEF) are proposed in the following section.

III. DEVELOPMENT OF GENERAL ENERGY FILTERS AND ENERGY QUALITY

A. DEFINITION OF GENERAL ENERGY FILTERS

In the signal processing, a **filter** is a device or process that removes some unwanted components or features from a signal. Filtering is a class of signal processing, the defined feature of filters being the complete or partial suppression of some aspect of the signal. **Power filters** are usually to remove some unwanted higher-frequency voltage or current components from a voltage or current waveform in the framework of Power Quality. A **general energy filter** is a filter that removes some unwanted zero-average power components from a power flow in the framework of Energy Quality. Power Quality is mainly concerned with the quality of voltage and current waveforms while Energy Quality is mainly concerned with the quality of power flow waveforms.

The general energy filter proposed in this paper can be implemented by a combination of the EES and its control. Depending on their different topology and order, there are different GEFs. In this section, the series, parallel, and series-parallel GEF are discussed in the 1st-order form. The 2nd-order series-parallel GEF is also discussed as an example of the high order case. For these cases, the energy conversion efficiency is assumed to be 100% and the storage loss is ignored. The effects of non-100% conversion efficiency on the GEF characteristics are discussed at the end of this section.

B. SERIES GEF (SGEF)

In a series GEF, the output power of the filter is directly controlled, which differs from the parallel GEF that will be discussed in Section III.C. It could be understood as the input fluctuating power goes into the energy storage device, which outputs a smoothed power to the rest of the system. The topology of a SGEF is presented in Fig. 3. Examples of the topology of SGEF could be a back-to-back VSC converter or a generator with rotor inertia as shown in the figure, where the DC-link capacitor and the rotor inertia play the role of energy storage.

Applying eq. (4) with the storage loss ignored, we have

$$E_0\frac{d\alpha}{dt} = P_S = P_{in} - P_{out} \tag{7}$$

The control law of P_{out} is proposed as

$$P_{out}^*(t) = \frac{E_0}{T}(\alpha(t) - \alpha_0) + P_0 \tag{8}$$

where α_0 and P_0 are the rated storage level and a roughly estimated long-term average output power respectively. P_0 could

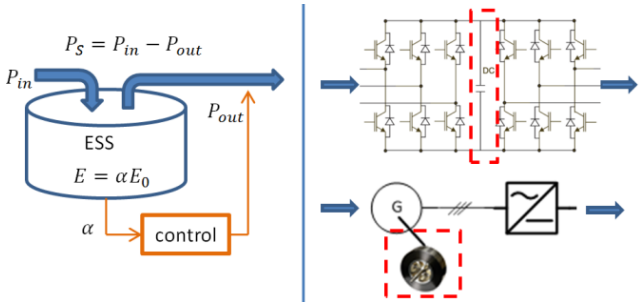

FIGURE 3. The topology and examples of the SGEF.

be obtained from the historical profile or other online/offline estimation methods, which is treated as a piece-wise constant here. We assume that the actual power tracks its reference fast enough so that $P^*_{out} = P_{out}$. Derivating eq. (8) and substitute it to eq. (7), we have

$$T\frac{dP_{out}}{dt} = P_{in} - P_{out} \tag{9}$$

$$\frac{P_{out}}{P_{in}} = \frac{1}{sT+1} \tag{10}$$

and according to eq. (8), the dependence of the storage level α to the output power and its sensitivity are

$$\alpha(t) = \frac{T}{E_0}(P_{out}(t) - P_0) + \alpha_0 \tag{11}$$

$$\frac{d\alpha}{dP_{out}} = \frac{T}{E_0} = \frac{1}{E_0\omega_0} \tag{12}$$

Eq. (10) is the transfer function of this 1st-order SGEF, where T is an arbitrarily set time constant. The control law of the output power is eq. (8), according to which only the storage level α needs to be measured. Eq. (11) guarantees the storage level swinging around its rated value, and eq. (12) shows how much α changes depending on the change of the output power, which is proportional to the inverse of E_0. In the SGEF, there is no measurement of the input power, which is a big advantage in many applications. It virtually works as a low-pass filter of the power flow with a cut-off frequency $\omega_0 = 1/T$. The input power exchanges its high-frequency fluctuation with the EES, and the output power is smoothed.

C. PARALLEL GEF (PGEF)

Compared with the series GEF, in a parallel GEF, the output power of the filter is not directly controlled. It could be viewed as the input fluctuating power does not go to the energy storage device, and the EES is connected to the power bus in parallel to compensate the high-frequency power fluctuation so that the total power output is smoothed. The topology and the power flow relationships are presented in Fig. 4. Examples of the topology of PGEF could be an inverter-based battery or flywheel storage system that is commonly to be seen nowadays.

Since the PGEF doesn't directly control P_{out}, the measurement of the input power is inevitable. Depending on weather

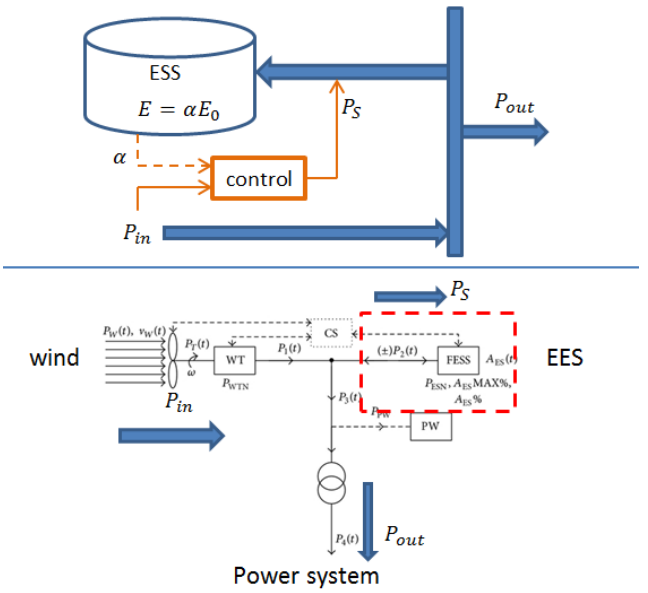

FIGURE 4. The topology and examples of the PGEF.

the measurement of the storage level α is also required by the controller, there are two possible control laws of P_S.

1) SINGLE-MEASURED CONTROL

This control method measures P_{in} only and does not measure α nor need to know the parameter E_0. As a cost, it has no control of α.

Based on Fig. 4, the power flows follow eq. (7) as well. In this case, the controlled power is no longer P_{out} but P_S. The control law of P_S is proposed as

$$P^*_S(t) = \left(1 - \frac{1}{Ts+1}\right) * P_{in}(t) \tag{13}$$

Again we assume the inner loops are fast enough so that $P_S = P^*_S$. From eq. (7) and (13), the transfer function of PGEF can be derived as the same as that shown in eq. (10). However, only the derivative of the storage level α can be obtained.

$$E_0\frac{d\alpha}{dt} = T\frac{dP_{out}}{dt} \tag{14}$$

$$\alpha = \frac{T}{E_0}P_{out} + \alpha_{ini} \tag{15}$$

After integration, there is a constant α_{ini}, the initial storage level, which is uncontrollable and vulnerable to disturbances. It suggests that this control method is not applicable without additional α monitoring and protection modules.

However, this control is simple and particularly useful in the kind of PGEF where there is no EES. More details are presented in section VI. A.

2) DOUBLE-MEASURED CONTROL

This method requires the measurement of P_{in} and α, and also need to know the parameter E_0. Compared with the single-measured control, this method has a good control of

the storage level. It is similar with the control of SGEF, and the control law of P_S can be obtained by minus eq. (8) from P_{in} as

$$P_S^*(t) = -\left[\frac{E_0}{T}(\alpha(t) - \alpha_0) + P_0\right] + P_{in}(t) \quad (16)$$

The transfer function, the real-time α (t) and its sensitivity under this control law are the same as shown in eq. (10)(11)(12) respectively.

One way to estimate P_0 is to assume it is equal to the long-term average value of P_{in}. Accordingly, the control law eq. (16) can be re-written as

$$P_0 = \frac{1}{T_{in}s + 1} * P_{in}(t) \quad (17)$$

$$P_S^*(t) = -\frac{E_0}{T}(\alpha(t) - \alpha_0) + \left(1 - \frac{1}{T_{in}s + 1}\right) * P_{in}(t) \quad (18)$$

where T_{in} is the input-averaging time constant which is much bigger than T.

D. SERIES-PARALLEL GEF (SPGEF)

Either in SGEF or PGEF, there is only one channel of the input unstable power. By contrast, in a series-parallel GEF, which can be viewed as an over position of them two, there are two channels of the unstable power. The topology of it is presented in Fig. 5. In this structure, the series channel is a SGEF, whose output power $P_{out,s}$ is directly controlled, and the parallel channel is for the direct connection of other unstable power to the bus without additional EES. The total output power P_{out} is smoothed as the output of this GEF. Since no EES is used deliberately for the parallel channel, the SPGEF is useful for building a large system with reduced hardware and cost.

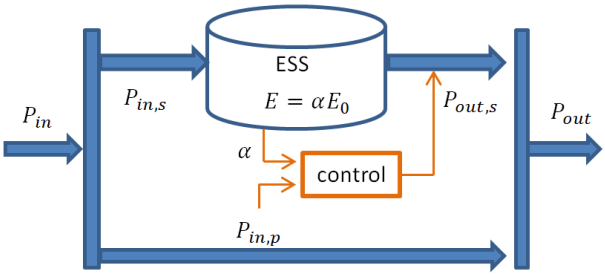

FIGURE 5. The topology of the SPGEF.

The control law of $P_{out,s}$ is proposed as

$$P_{out,s}^*(t) = \left[\frac{E_0}{T}(\alpha(t) - \alpha_0) + P_0\right] - P_{in,p}(t) \quad (19)$$

This control law is similar with the double-measured control of PGEF shown in eq. (16), in which also the measurement of α and $P_{in,p}$ are necessary and the parameter E_0 need to be known. On the other hand, the power through the series channel $P_{in,s}$ does not need to be measured, which is a similar feature with the SGEF. By assuming $P_{out,s}^*(t) = P_{out,s}(t)$ and applying eq. (7), it can be easily derived that the transfer function, the real-time α (t) and its sensitivity of the SPGEF are the same as shown in eq. (10)(11)(12) respectively.

E. 2nd-ORDER SPGEF

All the GEFs discussed above are of 1st order. In this subsection, the control law of a 2nd-order SPGEF is presented as an example of high order GEF.

Regarding Fig. 5, in the s-domain, the control law of $P_{out,s}$ is proposed as

$$P_{out,s}^*(t) = \left[\frac{E_0}{2T}\left(\frac{1}{Ts+1}\cdot\alpha(t) - \alpha_0\right) + P_0\right] - P_{in,p}(t) \quad (20)$$

By assuming $P_{out,s}^*(t) = P_{out,s}(t)$ and applying eq. (7), it is derived that the transfer function of this 2nd-order energy filter is

$$\frac{P_{out}}{P_{in}} = \frac{\frac{1}{2T^2}}{s^2 + \frac{s}{T} + \frac{1}{2T^2}} \quad (21)$$

It is in the standard form of a 2nd-order filter with its cut-off frequency (natural frequency) $\omega_0 = 1/\sqrt{2}T$ and damping ratio $\xi = 1/\sqrt{2}$. This damping ratio is the minimum value that guarantees no resonance, which also can be selected as other values in cases of need.

The steady-state storage level α depends on the total output power as

$$\alpha = \frac{2T}{E_0}(P_{out} - P_0) + \alpha_0 \quad (22)$$

and its sensitivity to the output power is

$$\frac{d\alpha}{dP_{out}} = \frac{2T}{E_0} = \frac{\sqrt{2}}{E_0\omega_0} \quad (23)$$

Compared with the 1st-order filter, it is known that the 2nd-order filter gives better smoothing effect, which is demonstrated in section IV. As a cost, it has a larger sensitivity of the storage level to the output power with the same cut-off frequency ω_0.

F. EFFECTS OF THE CONVERSION LOSS

In this subsection, the effects of the conversion loss on the characteristics of GEFs are discussed. Considering the conversion loss as indicated in eq. (5), the dynamic of the storage level becomes from eq. (7) to

$$\frac{E_0}{k_\eta}\cdot\frac{d\alpha}{dt} = E_0'\frac{d\alpha}{dt} = P_{in} - P_{out} \quad (24)$$

$$k_\eta = \begin{cases} \eta_c & charging \\ \frac{1}{\eta_d} & discharging \end{cases} \quad (25)$$

As can be seen, the equivalent effect of the conversion loss is to make the equivalent rated stored energy E_0' unknown and change between two values. Its average $\overline{E_0'} \in [\eta_d E_0, \frac{E_0}{\eta_c}]$. Its physical meaning can be interpreted as:

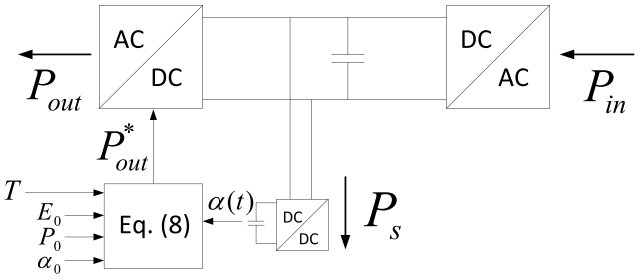

FIGURE 6. The topology and control of a supercapacitor-based SGEF.

when the EES charges/discharges power, the equivalent inertia, or the storage capacity, becomes bigger/smaller. Simulation results give that when the conversion efficiency is high enough (>90%), $\overline{E}_0^{'}$ can be approximated by E_0 without significant impacts on the GEF. This condition is usually met by the light storage. However, in cases such as the pumped-hydro and compressed air storage where the conversion efficiency is much lower, the uncertainty of $E_0^{'}$ need to be specially treated, for example, using adaptive control methods.

IV. TIME-DOMAIN SIMULATIVE DEMONSTRATIONS OF GEF

This section demonstrates the proposed series, parallel, and series-parallel GEF using RTDS simulation results. For each GEF, its hardware structure, time series of the input power, output power, and the storage level are presented. Each kind of GEF can be implemented based on different EES, yet to save this paper from trivial combinations of all possibilities, each GEF is implemented on one single but different EES with different input power waveform in different orders to show a variety of GEF application scenarios.

A. 1st-ORDER SUPERCAPACITOR-BASED SGEF

The SGEF is implemented based on a supercapacitor energy storage that is coupled to the DC link of a back-to-back converter as shown in Fig. 6. The rated stored energy $E_0 = \frac{1}{2}CV_c^2$ is 0.22kWh with $C = 100mF$ and $V_c = 4kV$. The input power is formulated as a single-frequency sinewave with exactly the cut-off frequency 0.5Hz of the GEF added to a DC component. The EES is controlled to maintain the DC-link voltage, thus there would be no energy variation of the DC capacitor and the difference between input andoutput power is balanced by the supercapacitor. The GEF control is applied to the output power, forming the whole system as an SGEF. Fig. 7 shows the waveform of the input and output power, which is the typical time-domain response of a low-pass filter with a 45 degree phase shift between them. Fig. 8 shows the storage level of the supercapacitor. Quantitative demonstration of the Bode plot is presented in section V.

B. 1st-ORDER BATTERY-BASED PGEF

The PGEF is implemented based on a battery storage system parallel connected with an unstable power source which in this case is represented by an induction generator, as shown in

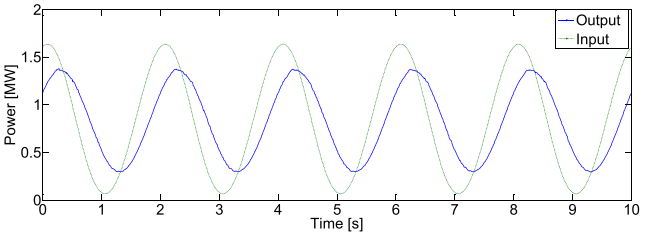

FIGURE 7. Input and output power of the SGEF. $f_{in} = f_{cut}$.

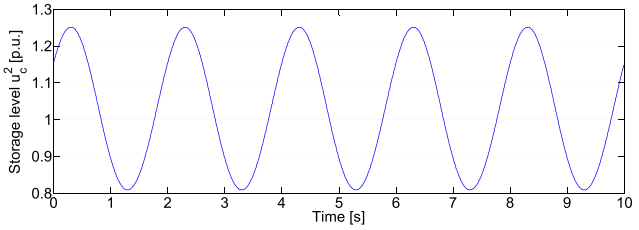

FIGURE 8. Storage level: the square of per-unit capacitor voltage of EES.

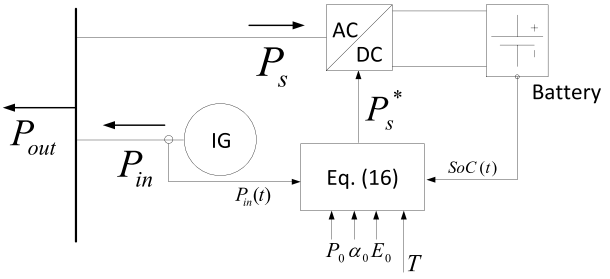

FIGURE 9. The topology and control of a battery-based PGEF.

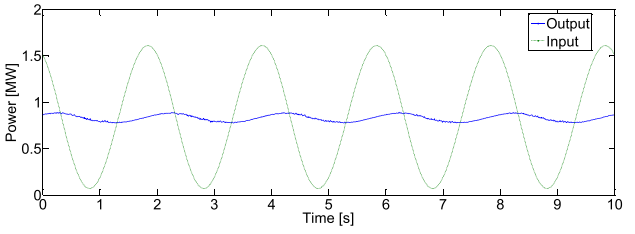

FIGURE 10. Input and output power of the PGEF. $f_{in} = 10f_{cut}$.

Fig. 9. The rated stored energy E_0 of the battery is 0.60kWh. A biased single-frequency torque similar with that in the subsection A is applied to the generator for testing and the input frequency is set to be 10 times bigger than the cut-off frequency 0.05Hz. Fig. 10 and 11 show the time series of the power flow and the storage level (SoC) of the battery, respectively. Results show that the high-frequency power fluctuation is very much suppressed in the output.

Compared with other EES solutions, the storage level of battery cannot be over 1.0 since the battery cannot be over charged. This can be guaranteed by the appropriate selection of P_0 in eq. (16). For a given application case, this feature means the rated stored energy E_0 of battery must be larger than that of other light storage methods.

C. 1st & 2nd-ORDER FLYWHEEL-BASED SPGEF

The SPGEF is implemented based on rotor flywheel storage with both 1st and 2nd- order control as shown in Fig. 12.

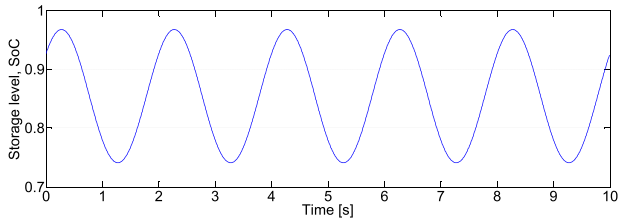

FIGURE 11. Storage level: *SoC* of the battery.

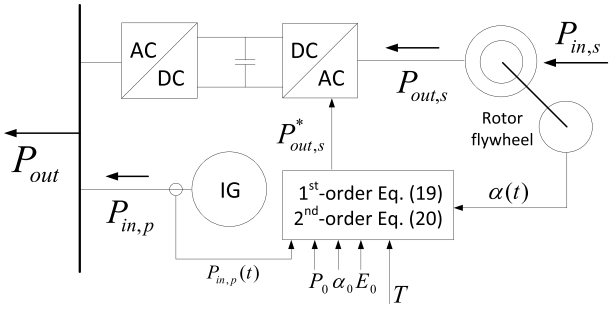

FIGURE 12. The topology and control of a rotor flywheel-based SPGEF.

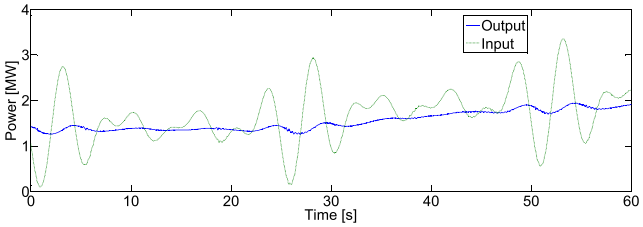

FIGURE 13. Total input and output power of the 1st-order SPGEF.

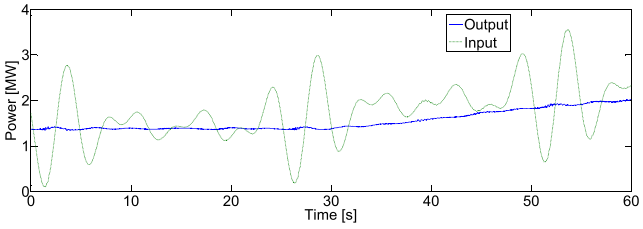

FIGURE 14. Total input and output power of the 2nd-order SPGEF.

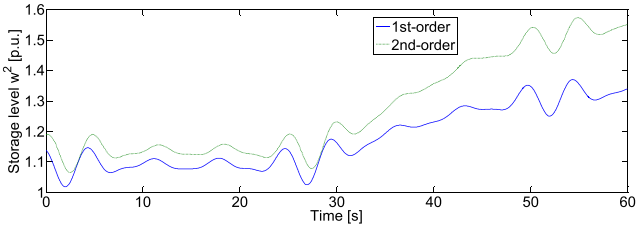

FIGURE 15. Storage level: the square of per-unit rotor speed of EES.

The series and parallel channel is the input of the induction machine with and without the rotor flywheel respectively. The rated stored energy E_0 of the rotor flywheel is 1.94kWh. In this case, a 60s real-time fluctuating power is injected to both the series and parallel channel to simulate the intermittent power generation, whose dc component has a step rise of 25% at t = 25s. The cut-off frequency is set to be

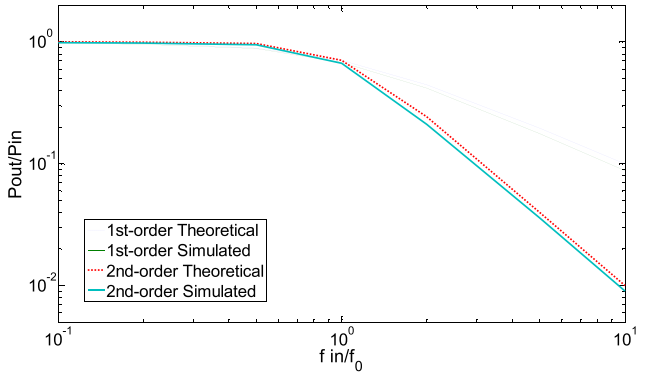

FIGURE 16. Bode plot: magnitude response of 1st and 2nd-order GEF.

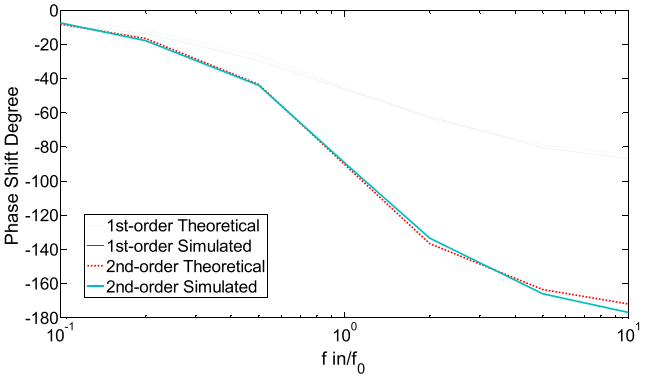

FIGURE 17. Bode plot: phase response of 1st and 2nd-order GEF.

0.02Hz, and the spectrum of the input power is centralized around 0.2Hz.

Fig. 13 and 14 show the time series of the power flow of the 1st and 2nd order SPGEF, respectively. Fig. 15 shows their storage levels. The results demonstrate that the GEF output is smoothed and tracking the dc component of the unknown total input power with both control methods. It can also be observed that the storage level increases with the step rise of the total input power. By contrast, the 2nd-order GEF has a better smoothing effect at the cost of a larger storage level sensitivity as indicated in eq. (23).

V. BODE PLOTS OF GEF

The frequency-domain demonstrations of both 1st and 2nd-order GEF are presented in their Bode plots as shown in Fig. 16 and 17. The data is obtained through RTDS simulations conducted on the flywheel-based SPGEF as discussed in IV.C with the cut-off frequency $f_0 = 0.1Hz$. The theoretical lines are drawn according to eq. (10) and (21), respectively, for comparisons. It can be seen that the simulation results match the theory very well. It is noticed that the simulated magnitude-frequency response is marginally smaller than the theory due to the energy losses in the system.

The results demonstrate that the proposed GEFs virtually work as low-pass filters to its input power.

VI. DESIGN OF GEF

This section briefly discusses the design process of GEF in practical applications based on the above knowledge. There

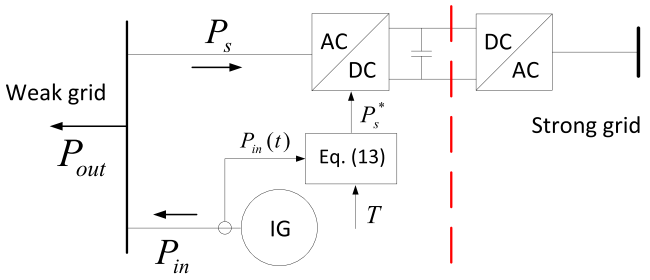

FIGURE 18. Example of a single-measured PGEF without EES.

are three key factors in designing a GEF: topology, control parameters, and the EES selection.

A. SELECTION OF TOPOLOGY

The topology of a GEF is selected based on the trade-off between the cost of power measurements and that of the extra power conversion capacity.

SGEF is a desired topology for it completely avoids the measurement of the input power. As a cost, it requires a controllable, full-rated energy conversion device so that the EES is able to directly control the total output power. In some cases, this can be conveniently achieved by applying and enlarging the inherent inertia of the energy conversion device itself. Examples include the rotor inertia of variable speed generators and the DC-link capacitors of back-to-back converters. In these applications, the full-rated conversion device is originally part of the system thus it raises no significant extra cost. In other cases where there is no original controllable full-rated conversion device, the trade-off must be made between its cost and the benefit of getting rid of the power measurement.

Double-measured PGEF has to measure the input power, while the advantage is its energy conversion device exchanges only the compensating power with the bus thus can be smaller scaled. Single-measured PGEF has no control of the storage level so it's not good for an EES-based system. Yet as indicated in III. B, it is useful in controlling the PGEF without EES where the compensating power is from another power source. An example is shown in Fig. 18. The weak grid side converter is using GEF control, and the fluctuating power is equivalently transferred to the strong grid.

SPGEF is a complex solution combining the advantages of both the above two (SGEF & PGEF). In this solution the total input power could be divided into series and parallel input. No measurement of the series input is required, while the parallel input does not go through the energy conversion device.

B. CONTROL PARAMETERS DETERMINATION

The control law of the GEF is determined by 4 parameters: T, α_0, P_0 and E_0. The first three can be arbitrarily set while the last one is related to the EES and fixed once it is implemented.

T is the most important parameter which determines the transfer function and the cut-off frequency of the GEF. The selection of it depends on the spectrum of the input fluctuating power and how fast the GEF is supposed to track the average.

Once T is set, E_0 is solely determined by the acceptable storage level sensitivity according to eq. (12) or (23). A bigger, slower input power change needs an EES with bigger E_0 to keep the storage level within the safe range.

α_0 is normally set to be 1.0 to fully use the capacity of EES. However, when the EES (e.g. battery) cannot be over charged, 1.0 is the maximum of α, so α_0 should be somewhere lower than 1.0.

P_0 is the rated capacity of the unstable input power.

C. SELECTION OF EES

First of all, the EES must be able to provide sufficient E_0. It very much depends on the spectrum and the magnitude of fluctuations of the input power. As discussed in section II, different EES is with different typical range of E_0, which is to be selected accordingly.

It is also worth considering that a suitable EES should be compatible with the power source in the GEF system. Rotor flywheel is compatible with a rotating machine, while the voltage source storage such as the battery or supercapacitor is more desired with solar power generation.

VII. CONCLUSIONS

In this paper, the concept of filter widely used in the area of signal processing has been, to the best knowledge of authors, applied to power flow control in the technical framework of energy quality for the first time. The proposed general energy filters (GEF) are able to smooth, track and process fluctuating input power flows using energy storage to largely improve the energy quality of their output powers. Before developing GEFs, the current mainstream electrical energy storage (EES) methods have been briefly reviewed and classified into light and heavy storage groups. A power-based general model has been proposed to describe all EES in a unified framework. Based on this model, the implementation schemes of the series, parallel, and series-parallel GEF have been proposed and demonstrated in the time-domain simulations on RTDS with different EES and input power characteristics, respectively. Their topologies, control methods, transfer functions, and storage level sensitivities have been studied in details.

Frequency-domain analysis results have demonstrated that GEF virtually work as low-pass energy filters, whose orders and transfer functions can be arbitrarily designed. Comparatively, the 2nd-order GEF have better power smoothing effects than that of the 1st-order GEF, yet at a cost of higher storage level sensitivity.

Finally, it has been discussed that in order to design GEF systems for practical applications, their topologies, control parameters and EES are 3 key factors that need to be considered.

REFERENCES

[1] P. Malysz, S. Sirouspour, and A. Emadi, "An optimal energy storage control strategy for grid-connected microgrids," *IEEE Trans. Smart Grid*, vol. 5, no. 4, pp. 1785–1796, Jul. 2014.
[2] M. R. Sandgani and S. Sirouspour, "Coordinated optimal dispatch of energy storage in a network of grid-connected microgrids," *IEEE Trans. Sustain. Energy*, vol. 8, no. 3, pp. 1166–1176, Jul. 2017.
[3] A. K. Barnes, J. C. Balda, and A. Escobar-Mejía, "A semi-Markov model for control of energy storage in utility grids and microgrids with PV generation," *IEEE Trans. Sustain. Energy*, vol. 6, no. 2, pp. 546–556, Apr. 2015.
[4] X. Zhao, Z. Yan, and X.-P. Zhang, "A wind-wave farm system with self-energy storage and smoothed power output," *IEEE Access*, vol. 4, pp. 8634–8642, 2016.
[5] M. A. Eltawil and Z. Zhao, "Grid-connected photovoltaic power systems: Technical and potential problems—A review," *Renew. Sustain. Energy Rev.*, vol. 14, no. 1, pp. 112–129, 2010.
[6] A. Blavette, D. L. O'Sullivan, R. Alcorn, T. W. Lewis, and M. G. Egan, "Impact of a medium-size wave farm on grids of different strength levels," *IEEE Trans. Power Syst.*, vol. 29, no. 2, pp. 917–923, Mar. 2014.
[7] J. Neely, L. Rashkin, M. Cook, D. Wilson, and S. Glover, "Evaluation of power flow control for an all-electric warship power system with pulsed load applications," in *Proc. IEEE Appl. Power Electron. Conf. Expo. (APEC)*, Long Beach, CA, USA, Mar. 2016, pp. 3537–3544.
[8] T. Ma, M. H. Cintuglu, and O. A. Mohammed, "Control of a hybrid AC/DC microgrid involving energy storage and pulsed loads," *IEEE Trans. Ind. Appl.*, vol. 53, no. 1, pp. 567–575, Jan./Feb. 2017.
[9] Á. Ortega and F. Milano, "Modeling, simulation, and comparison of control techniques for energy storage systems," *IEEE Trans. Power Syst.*, vol. 32, no. 3, pp. 2445–2454, May 2017.
[10] H. M. Hasanien, "A set-membership affine projection algorithm-based adaptive-controlled SMES units for wind farms output power smoothing," *IEEE Trans. Sustain. Energy*, vol. 5, no. 4, pp. 1226–1233, Oct. 2014.
[11] F.-J. Lin, H.-C. Chiang, J.-K. Chang, and Y.-R. Chang, "Intelligent wind power smoothing control with BESS," *IET Renew. Power Generat.*, vol. 11, no. 2, pp. 398–407, 2017.
[12] A. M. Howlader, T. Senjyu, and A. Y. Saber, "An integrated power smoothing control for a grid-interactive wind farm considering wake effects," *IEEE Syst. J.*, vol. 9, no. 3, pp. 954–965, Sep. 2015.
[13] I. Ngamroo and T. Karaipoom, "Cooperative control of SFCL and SMES for enhancing fault ride through capability and smoothing power fluctuation of DFIG wind farm," *IEEE Trans. Appl. Supercond.*, vol. 24, no. 5, Oct. 2014, Art. no. 5400304.
[14] T. I. Bø and T. A. Johansen, "Battery power smoothing control in a marine electric power plant using nonlinear model predictive control," *IEEE Trans. Control Syst. Technol.*, vol. 25, no. 4, pp. 1449–1456, Jul. 2017.
[15] Z. Zhou, F. Scuiller, J. F. Charpentier, M. El Hachemi Benbouzid, and T. Tang, "Power smoothing control in a grid-connected marine current turbine system for compensating swell effect," *IEEE Trans. Sustain. Energy*, vol. 4, no. 3, pp. 816–826, Jul. 2013.
[16] T. Martinsen *et al.*, "Improved grid operation through power smoothing control strategies utilizing dedicated energy storage at an electric vehicle charging station," in *Proc. CIRED Workshop*, Helsinki, Finland, 2016, pp. 1–4.
[17] X. Luo, J. Wang, M. Dooner, and J. Clarke, "Overview of current development in electrical energy storage technologies and the application potential in power system operation," *Appl. Energy*, vol. 137, pp. 511–536, Jan. 2015.
[18] D. O. Akinyele and R. K. Rayudu, "Review of energy storage technologies for sustainable power networks," *Sustain. Energy Technol. Assessments*, vol. 8, pp. 74–91, Dec. 2014.
[19] A. H. Slocum, G. E. Fennell, G. Dundar, B. G. Hodder, J. D. C. Meredith, and M. A. Sager, "Ocean renewable energy storage (ORES) system: Analysis of an undersea energy storage concept," *Proc. IEEE*, vol. 101, no. 4, pp. 906–924, Apr. 2013.
[20] S. Jafarishiadeh, M. Farasat, and A. M. Bozorgi, "Modeling, analysis and design of an undersea storage system," in *Proc. IEEE Energy Convers. Congr. Expo. (ECCE)*, Milwaukee, WI, USA, Sep. 2016, pp. 1–6.
[21] N. M. Dimitrijevic, "Role of water and carbonates in photocatalytic transformation of CO_2 to CHP_4 on titania," *J. Amer. Chem. Soc.*, vol. 133, no. 11, pp. 3964–3971, 2011.
[22] T. Desrues, J. Ruer, P. Marty, and J. F. Fourmigué, "A thermal energy storage process for large scale electric applications," *Appl. Thermal Eng.*, vol. 30, no. 5, pp. 425–432, 2010.
[23] W. Chang, "The state of charge estimating methods for battery: A review," *ISRN Appl. Math.*, vol. 2013, Jul. 2013, Art. no. 953792.

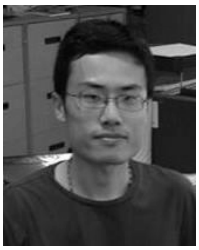

ZUANHONG YAN was born in Nanjing, China, in 1990. He received the B.Eng. degree from the Huazhong University of Science and Technology, Wuhan, China, and the University of Birmingham, Birmingham, U.K., in 2012, and the M.Sc. degree from the University of Manchester, Manchester, U.K., in 2013. He is currently pursuing the Ph.D. degree with the University of Birmingham. His research interests include renewable energy conversion and integration, wind/wave farm system, and energy storage control.

XIAO-PING ZHANG (M'95–SM'06) received the B.Eng., M.Sc., and Ph.D. degrees in electrical engineering from Southeast University, China, in 1988, 1990, and 1993, respectively. He was an Associate Professor with The University of Warwick, U.K. He was with the China State Grid EPRI (NARI Group) on EMS/DMS advanced application software research and development from 1993 to 1998. From 1998 to 1999, he was visiting UMIST. From 1999 to 2000, he was an Alexander-von-Humboldt Research Fellow with the University of Dortmund, Germany. He is currently a Professor of electrical power systems with the University of Birmingham, U.K. He is also the Director of Smart Grid, Birmingham Energy Institute, and the Co-Director of the Birmingham Energy Storage Center. He has co-authored the first and second edition of the monograph *Flexible AC Transmission Systems: Modeling and Control* (Springer, 2006 and 2012). He has co-authored the book *Restructured Electric Power Systems: Analysis of Electricity Markets with Equilibrium Model* (IEEE Press/Wiley, 2010). He pioneered the concept of Global Power and Energy Internet, Energy Union, UK's Energy Valley.